# Investigating the Physics of Rotor Vortex Ring State using the Vorticity Transport Model

Gary A. Ahlin* and Richard E. Brown†
Department of Aeronautics, Imperial College
London, United Kingdom.

## Abstract

Some of the root causes of the behaviour of a helicopter rotor in the vortex ring state are investigated using simulations, conducted using Brown's Vorticity Transport Model, of a two-bladed teetering rotor descending into the vortex ring state under conditions of constant collective pitch. Contrary to some previous reports, the onset of thrust settling on the rotor is found to occur at descent rates much lower than that at which the wake breaks down into the toroidal form that is characteristic of the fully developed vortex ring state. Thrust settling is caused by a loss of loading on the outboard parts of the rotor that is induced initially by compression of the wake below the rotor during low-speed descent. The behaviour of the rotor in the vortex ring state appears to be practically insensitive to the twist of the blades, at least for rotors with moderate levels of blade twist. Although blade stall has little effect on the onset of the vortex ring state, it is quite likely that stall on the inner parts of the rotor, even for rotors with moderate levels of blade twist, may modify significantly the behaviour of the system during the later stages of the development of the vortex ring state.

## Notation

| | |
|---|---|
| $A$ | : rotor disc area, $\pi R^2$ |
| $C_B$ | : blade sectional loading, scaled by $\frac{1}{2}\rho c(\Omega R)^2$ |
| $C_L$ | : blade sectional lift coefficient |
| $C_P$ | : rotor power, scaled by $\rho A(\Omega R)^3$ |
| $C_Q$ | : rotor torque, scaled by $\rho AR(\Omega R)^2$ |
| $C_{Qh}$ | : $C_Q$ measured under hovering conditions |
| $C_{Q0}$ | : rotor profile torque, scaled by $\rho AR(\Omega R)^2$ |
| $C_T$ | : rotor thrust, scaled by $\rho A(\Omega R)^2$ |
| $C_{Th}$ | : $C_T$ measured under hovering conditions |
| $c$ | : blade chord, scaled by $R$ |
| $N$ | : number of rotor blades |
| $R$ | : rotor radius |
| $t$ | : time, scaled by $1/\Omega$ |
| $\alpha_e$ | : blade sectional angle of attack |
| $\lambda_i$ | : rotor induced velocity, scaled by $\Omega R$ |
| $\overline{\lambda}_i$ | : $\lambda_i$, scaled by $\sqrt{C_T/2}$ |
| $\mu_z$ | : rotor descent rate, scaled by $\Omega R$ |
| $\overline{\mu}_z$ | : $\mu_z$, scaled by $\sqrt{C_T/2}$ |
| $\tilde{\mu}_z$ | : $\mu_z$, scaled by $\sqrt{C_{Th}/2}$ |
| $\rho$ | : air density |
| $\Sigma$ | : wake intensity |
| $\sigma$ | : rotor solidity, $Nc/\pi$ |
| $\Omega$ | : rotor angular velocity |

## Introduction

In all flight regimes, including axial flight, the helical structure of the wake of a helicopter rotor is inherently unstable to small perturbations in geometry or strength. The growth rate of disturbances to the rotor wake is, in part, a function of the pitch of the wake helix, or, in other words, to the relative spacing between adjacent vortex filaments (Ref. 1). The effect of the growth of these disturbances is to

*Postgraduate Research Assistant.
†Senior Lecturer. E-mail: r.e.brown@imperial.ac.uk
Presented at the 31st European Rotorcraft Forum, Florence, Italy, September 13-15, 2005. 

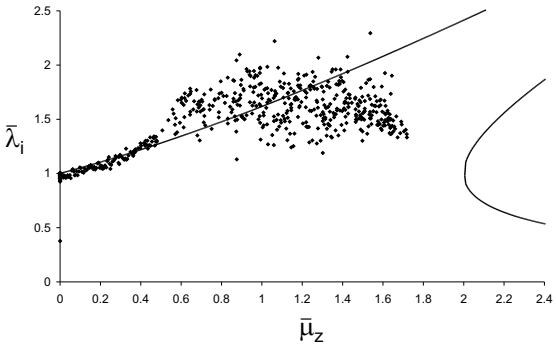


Figure 1: *Mean inflow vs. descent rate: VTM simulated data.*

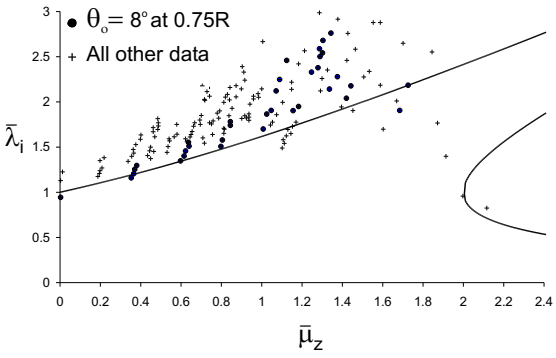


Figure 2: *Mean inflow vs. descent rate: Data from experiments of Washizu et al.*

disorganise the initially structured helical form of the rotor wake. Under normal flight conditions the breakdown of spatial order in the flow field occurs in the far field, some distance downstream of the rotor, and the growing disturbances to the wake are convected away from the rotor at a speed that is dependent on the rotor inflow and the free stream velocity (Ref. 2). In descending flight, however, the rate of convection of the perturbations to the wake becomes comparable to their global rate of expansion, and thus within a range of descent rates it becomes possible for the disturbances to reach the rotor (Refs. 2, 3). Within this range of descent rates the helical structure of the wake breaks down into a highly unsteady toroidal form known as the vortex ring state (VRS). Within the VRS the aerodynamic forces generated by the rotor fluctuate appreciably and erratically in response to the unsteady flow near to the rotor (Refs. 4, 5).

Particle Image Velocimetry (PIV) has shown (Ref. 6) that the global topology of the flow field at the onset of wake breakdown is highly transient, and that the topology of the wake at any particular instant may be quite different to the topology of the mean flow. At the onset of the VRS, where the descent rate is approximately half of the rotor downwash velocity, PIV shows the wake to swap intermittently between two forms - one of which is similar to the structure found at hover, and another that resembles a ring, or toroid, of vorticity that bundles up beneath the rotor plane. As the descent rate is increased to near the mean rotor downwash velocity the wake structure becomes more inclined to remain in the second state and thus the rotor appears to be engulfed in the recirculating flow that is characteristic of the VRS. The unsteadiness of this recirculating flow arises from a recurrent, aperiodic, and spatially non-uniform process in which the vorticity within the ring builds up over a number of rotor revolutions and then is ejected into the flow downstream of the rotor (Refs. 2, 3, 7, 8). In addition to the highly transient blade loading, the initial concentration of vorticity near to the rotor during the onset of VRS causes a reduction in the thrust produced by the rotor if the collective pitch setting is held constant (Refs. 4, 9), or equivalently an increase in the power required by the rotor if the thrust is held constant (Ref. 10). This effect, known as ‘thrust settling’ or ‘settling with power’, depending on context, persists until the descent rate becomes large enough so that the recirculating flow near the rotor can no longer be sustained and the orderly structure of the wake near to the rotor is re-established (Ref. 11).

The behaviour of a rotor operating within a field of concentrated and highly disorganised vorticity is strongly non-linear. The physics of the growth and transmission of disturbances through the rotor wake is extremely complex, and any attempt to understand these processes is complicated by the presence of long-range interactions between evolving vortex filaments and coupling between the dynamics of the wake and the loading produced on the rotor. The

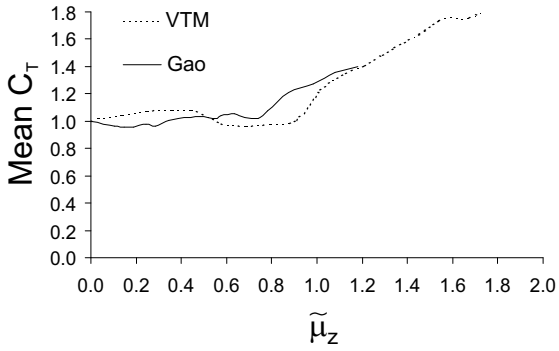


Figure 3: *Mean thrust vs. descent rate: VTM simulation and Gao's experimental data.*

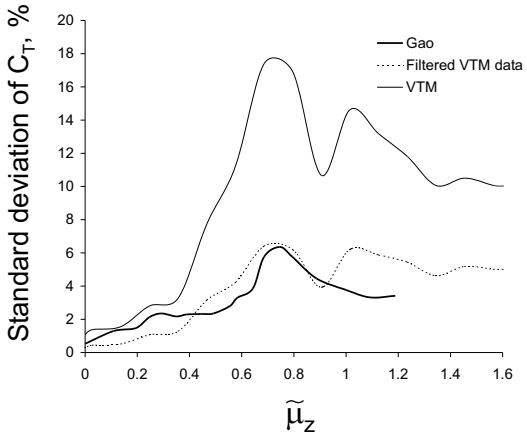


Figure 4: *Standard deviation of thrust fluctuations vs. descent rate: VTM simulation and Gao's experimental data.*

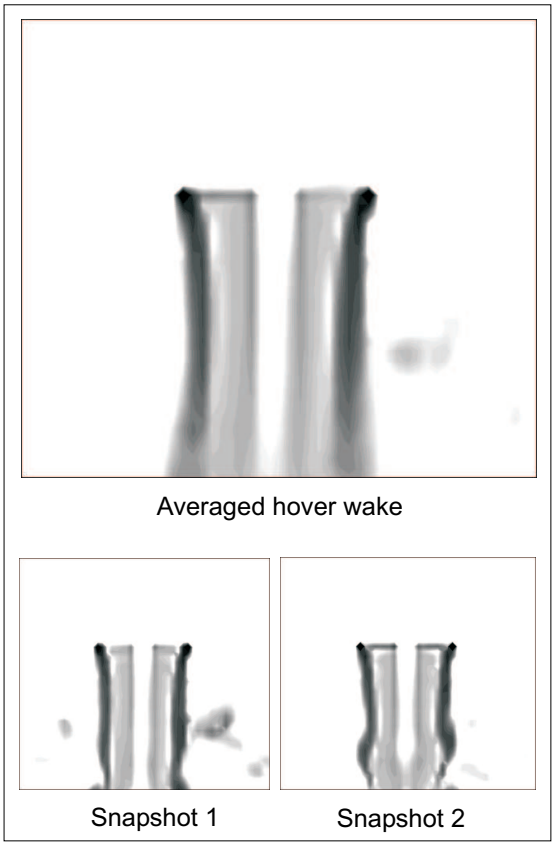


Figure 5: *VTM wake geometry at hover.*

## The Vorticity Transport Model

complexity of the VRS is borne out by varied and sometimes unintuitive and conflicting reports, as revealed in Johnson's survey of the published VRS literature (Ref. 12). Such is the difficulty in observing or modelling the physics of the VRS that few of the characteristic features of this flow state have been satisfactorily explained at a fundamental level, although much progress has been made in recent years. The present work attempts to contribute to the body of knowledge concerning the fundamental mechanisms at work within the VRS by using the Vorticity Transport Model (VTM), developed by Brown and Line (Refs. 13, 14) to model the flow numerically. In particular, the causes of thrust settling are investigated, and the influence of *moderate* blade twist on the dynamics of the wake and the subsequent performance of a rotor in descent are scrutinised.

The Vorticity Transport Model (VTM) employs a direct computational solution of the incompressible Navier-Stokes equations, expressed in vorticity-velocity form, to simulate the evolution of the wake of a helicopter rotor. The key to the method is the use of a CFD-type vorticity-conserving algorithm to evolve the governing equations through time. The algorithm is implemented on a mesh of computational cells that continually adapts its structure to capture the evolving structure of the vorticity field created by the rotor. In contrast to many other CFD-based approaches, the method is capable of maintaining the spatial localization of vortical structures in the flow for very long computational times. This property makes the VTM highly suitable for VRS calculations, since a large proportion of the vorticity generated under VRS conditions remains close to the helicopter for very many rotor revolutions.

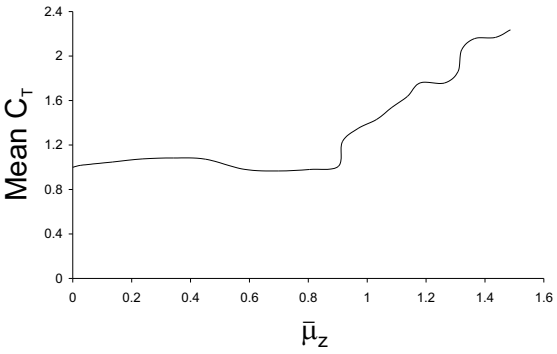


Figure 6: *Mean thrust vs. descent rate: VTM simulation of Gao's rotor.*

The VTM has been used previously to examine the onset and development of the VRS for isolated rotors (Ref. 3), some of the general effects of high rates of blade twist on rotor behaviour in the VRS (Ref. 15) and the influence of the fuselage and tail rotor on VRS onset (Ref. 16).

## Numerical Simulation of the VRS

In this section, the results of a numerical simulation of Gao's experimental configuration (Ref. 17) are compared with available data to show that the VTM is indeed capable of capturing the flow physics of the VRS to a reasonable degree of accuracy. Gao used two-bladed teetering rotors in his experiments; the rotor that was simulated had a solidity of 0.077, and blades with constant chord and 5.5° of linear twist from root to tip. In Gao's tests, the collective pitch was held constant at 10° (as measured at 70% span) while the descent speed of the rotor was varied. The attraction of Gao's experiment compared to the many other tests described in the literature is the simplicity of the rotor configurations that were tested together with the relatively low twist rates of the blades. This last point is important, as it avoids the issues of radial flow and the resultant stall delay that are thought to complicate the behaviour of more highly twisted blades. Gao's experiments have a further advantage in that they were conducted on a whirling tower, rather than in a wind tunnel, and

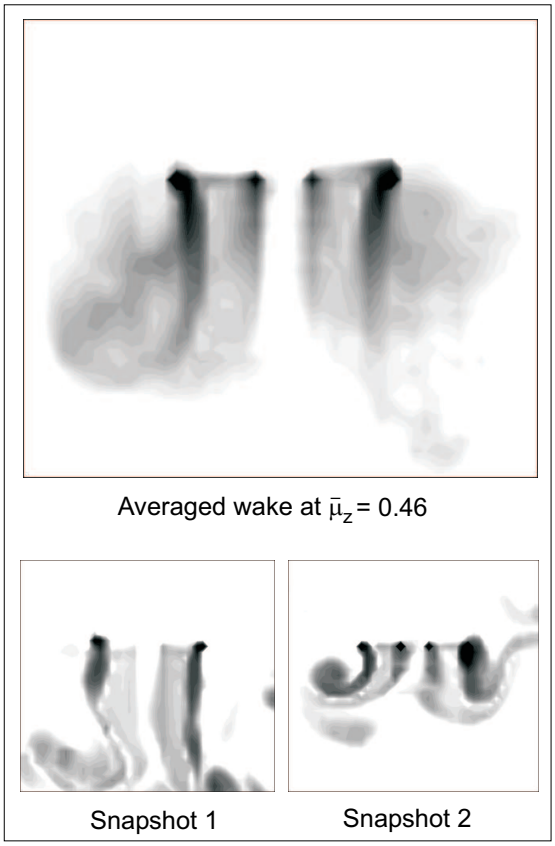


Figure 7: *VTM wake geometry at* $\overline{\mu}_z = 0.46$.

thus contamination by wind tunnel effects should be absent. Other physical effects associated with the whirling tower, such as centripetal forcing of the wake and gyroscopic effects on the rotor remain significant unknowns, however (despite Gao's conclusion that these effects would be negligible) and were not modelled in the VTM simulations. It is important to note that, in all of the VTM simulations discussed in the present work, the range of descent speeds of interest was traversed by flying the rotor at a constant, but small, rate of acceleration ($d\mu_z/dt = 2 \times 10^{-4}$ per rotor revolution). Acceleration is known to affect the onset and development of the VRS (Ref. 2), and this feature of the simulations, although likely to have only a small effect, must be borne in mind when considering the data.

Many of the classical references portray the effects of the VRS on rotor performance by presenting the variation with descent speed of the mean inflow

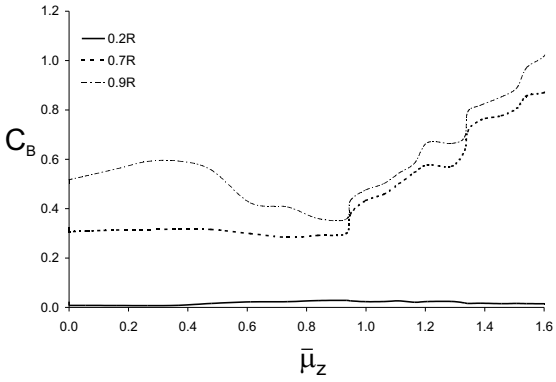


Figure 8: *Blade loading vs. descent rate at various stations along the blade.*

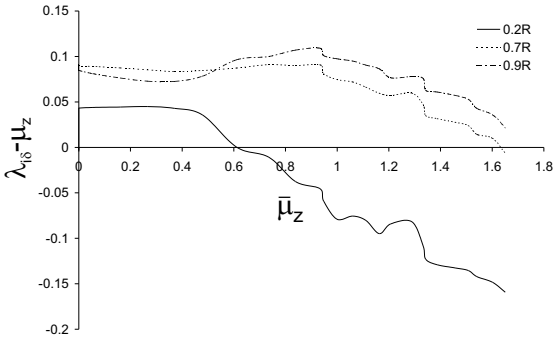


Figure 9: *Vertical flow velocity vs. descent rate at various stations along the blade.*

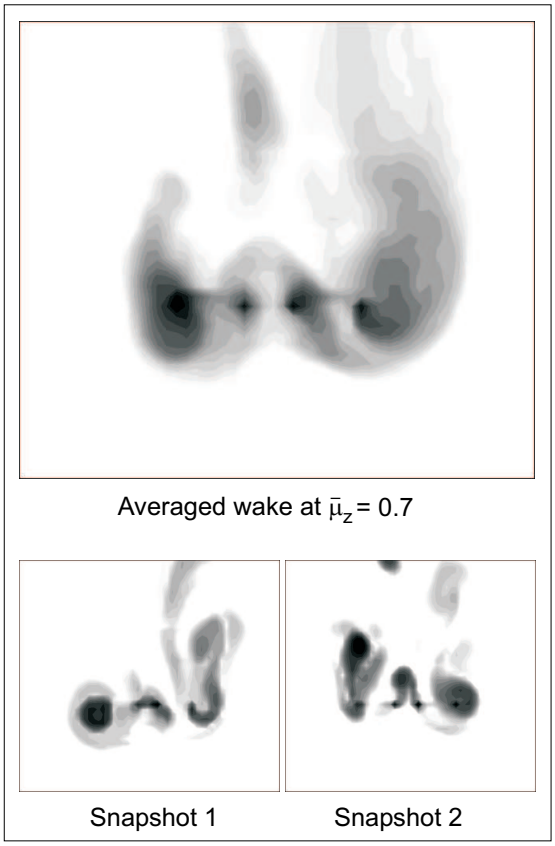


Figure 10: *VTM wake geometry at* $\overline{\mu}_z = 0.7$.

generated by the rotor. The difficulties involved in obtaining the inflow directly from experimental measurement are usually circumvented by deriving this information from measurements of rotor thrust and torque (Refs. 5, 10). The identical process can be applied to performance data obtained from the VTM, and predictions can be compared against experimental data for similar rotors.

The approach adopted to obtain the inflow from measurements of thrust and torque follows directly the technique used by Washizu *et al.* (Ref. 10). Firstly the profile torque of the rotor is estimated as

$$C_{Q0} = C_{Qh} - C_{Th}\lambda_h \tag{1}$$

where $C_{Qh}$ and $C_{Th}$ are the torque and thrust coefficients measured in hover, and $\lambda_h = \sqrt{C_{Th}/2}$. Then, assuming that the relationships

$$C_P = (C_Q - C_{Q0}) + C_T\mu_z \tag{2}$$

and

$$C_P = C_T\lambda_i \tag{3}$$

hold in descending flight, the inflow through the rotor is given by

$$\lambda_i = \left(\frac{C_Q - C_{Q0}}{C_T} + \mu_z\right) \tag{4}$$

This analysis assumes that the rotor inflow and blade loading is distributed uniformly across the rotor disk, and thus produces results that are somewhat at odds with direct measurements of velocity in the plane of the rotor.

Fig. 1 shows the variation of inflow, obtained using Eq. 4 from VTM simulations of the thrust and torque for Gao's rotor, plotted against non-dimensional descent rate $\overline{\mu}_z = \mu_z/\sqrt{C_T/2}$. For comparison, Fig. 2 shows experimental data obtained by Washizu *et al.* (Ref. 10) for a three bladed rotor with 8° of twist at various collective pitch settings. Within limits, the variation of inflow with descent

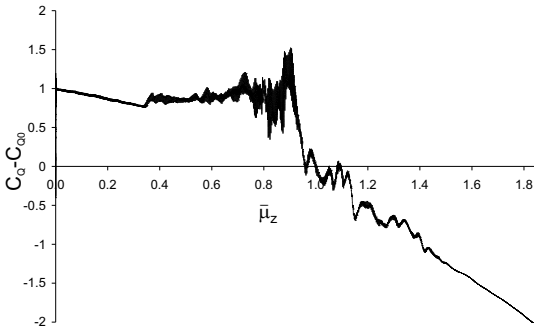


Figure 11: *VTM simulation of torque vs. descent rate with the rotor operating at constant mean thrust.*

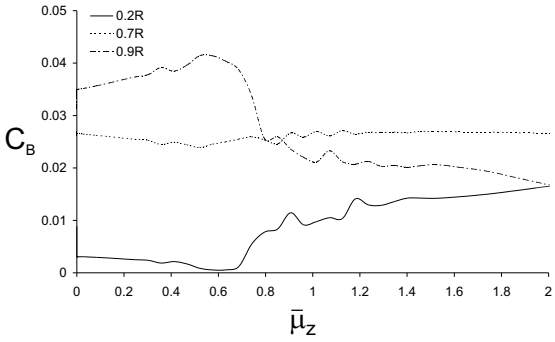


Figure 12: *Blade loading vs. descent rate at various stations along the blade with the rotor operating at constant mean thrust.*

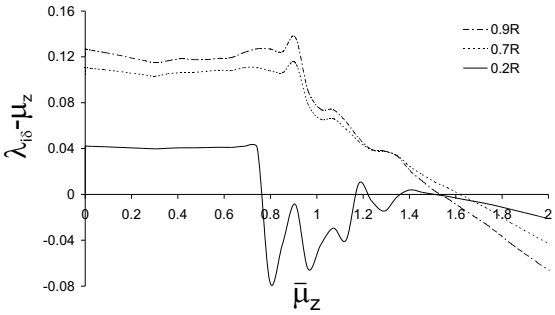


Figure 13: *Vertical flow velocity vs. descent rate at various stations along the blade with the rotor operating at constant mean thrust.*

rate is traditionally held to be a universal characteristic of the behaviour of all rotors within the VRS. Thus, even though the rotors used in the simulation and in Washizu's experiment are not directly comparable, the simulations capture well the broad characteristics of the measured variation of inflow with descent rate, as well as the extent and order of magnitude of the thrust perturbations experienced by the rotor during its transit through the VRS.

Figures 3 and 4 show direct comparisons between VTM simulations and Gao's experimentally obtained thrust data. The thrust signal is separated into a mean component and a superimposed fluctuation, and, to match with Gao's presentation of his own data, is plotted against non-dimensional descent rate $\tilde{\mu}_z = \mu_z/\sqrt{C_{Th}/2}$. The agreement between simulation and experiment for the mean thrust is both qualitatively and quantitatively reasonable, although there are some differences in detail. For instance, the thrust settling seen in Gao's data occurs over a smaller range of descent speeds than it does in the simulation. Interestingly, Gao's results show a dip in the mean $C_T$ during very low speed descent, which seems contrary to the predictions of momentum-based theories, whilst the simulation shows a more intuitive variation over the same range of descent rates.

The fluctuating component of the thrust is represented in Fig. 4 as the standard deviation of $C_T$ from the mean, expressed as a percentage of the mean $C_T$ at the same descent rate. Although the figure shows reasonable qualitative agreement between simulation and experiment, particularly with regards to the descent rate at which the fluctuations in rotor thrust attain their greatest amplitude, the fluctuations predicted by the VTM are significantly more severe than those measured in Gao's experiment. This observation is directly at odds with the results of the comparison against Washizu's data, where the amplitude of the thrust fluctuations, if anything, is underpredicted. It is easy to ascribe these discrepancies to the influence of rotor geometry on rotor behaviour in the VRS, but an important distinction between the simulation of Gao's experimental system and the real system itself is that the simulated thrust data were obtained by direct integration of the aerodynamic loading on the blades, whereas some degree of attenuation of the time-varying component of the experimental signal is inevitable given the impossibility of constructing an absolutely rigid

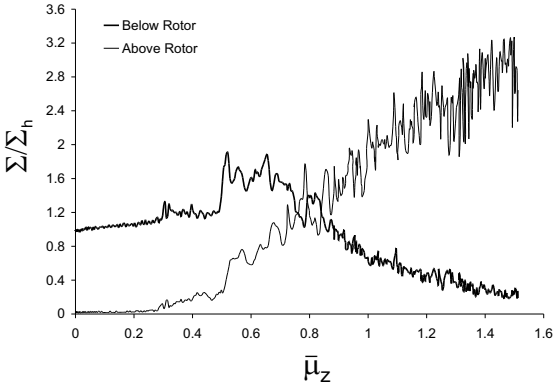


Figure 14: *Comparison of wake intensity above and below the rotor vs. descent rate.*

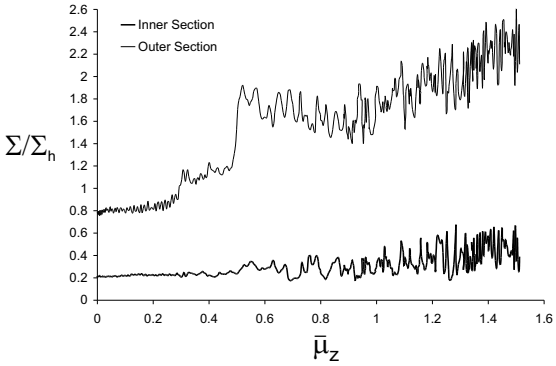


Figure 15: *Comparison of wake intensity inboard and outboard on the rotor vs. descent rate.*

experimental rig. Discussion, better still, quantification, of this effect is very rare in the experimental VRS literature. To emulate this effect, the experimental rig was modelled as a critically-damped simple harmonic system and the resulting transfer function was used to filter the computationally-generated thrust signal. As shown in Fig. 4, reasonable agreement between experiment and simulation is obtained if the experimental rig is assumed to have a natural frequency of about $6\Omega$.

The results presented here suggest that the VTM is capable of a reasonably good level of quantitative accuracy in predicting the aerodynamics and dynamics of rotors in descending flight. Validation is an ongoing process, however, and is certainly not aided by the paucity at present of rigorously-defined, self-consistent data of the quality and resolution required to properly validate modern computational codes.

# The Physics of Thrust Settling

A well-known aspect of experimental measurements on rotors flown at constant collective pitch into the VRS is the decrease in mean thrust that accompanies the onset of large-amplitude thrust fluctuations on the rotor. This phenomenon, known as thrust settling, has been observed in numerous experiments (Refs. 4, 9) but most authors have associated its onset with the envelopment of the rotor in the recirculating, toroidal flow of the fully-developed VRS. Yet, from simulations conducted with the VTM, it is clear that the onset of thrust settling occurs well before the wake has completely broken down into its toroidal VRS topology.

For later comparison, Fig. 5 shows a contour plot of the vorticity in the rotor wake, averaged over several rotor revolutions, with the rotor in hover. Several snapshots of the instantaneous configuration of the rotor wake at various arbitrary times are also shown for comparison. The role of the wake instability in the far field in destroying the coherence of the instantaneous geometry of the wake, or equivalently in dispersing the vorticity in the mean, can be seen clearly. Fig. 6 shows that thrust settling initiates at $\overline{\mu}_z \approx 0.46$, and Fig. 7 shows a similar diagram to Fig. 5 at this descent rate. It is clear from this set of images that, at the onset of thrust settling, the vorticity in the rotor wake is still being convected below the rotor, and, indeed, retains qualitatively much of the structure of the hovering rotor wake - even though the coherent portion of the wake tube has been truncated significantly by the dynamics of the disturbances in the wake. Thrust settling thus begins well before the rotor flow has collapsed into the toroidal form of the fully-developed VRS. The origin of thrust settling can be more clearly understood by examining the variation with descent rate of the spanwise distribution of loading along the rotor blades. Fig. 8 shows clearly that thrust settling is associated with a considerable fall in the loading only on the outboard sections of the blade. The inboard sections of the blade play only a small role in the thrust settling phenomenon and Fig. 8 sug-

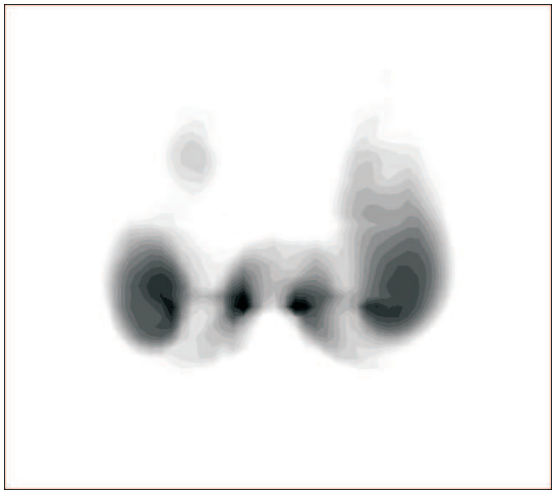

Figure 16: *Averaged wake geometry at* $\overline{\mu}_z = 0.8$.

Figure 17: *Averaged wake geometry at* $\overline{\mu}_z = 1.0$.

gests that the loading from the root of the blade out to $0.7R$ might even increase slightly at the onset of thrust settling. Fig. 9 shows the variation with descent rate of the velocity normal to the blade, as inferred from the computed effective angle of attack of the blade and corrected for the blade flap velocity. Comparison of Figs. 8 and 9 shows clearly that the reduction in loading on the blade tips is associated with an increase in the inflow that, at the onset of thrust settling, is also localised at the outer sections of the blades. A similar observation was made by Azuma and Obata (Ref. 9), who were able to measure the inflow at several radial stations under their experimental rotor using small, responsive windmill type anemometers. In the absence of direct observations of the structure of the rotor wake, they concluded that the increase in inflow resulted from the rotor being enveloped in the toroidal flow of the fully developed VRS. The localised nature of the thrust decrement associated with thrust settling suggests, however, that a much more local flow effect is responsible for the phenomenon than the large-scale flow disturbance associated with the fully-developed VRS. Indeed, simulations confirm that the toroidal flow of the fully developed VRS (as illustrated in Fig. 10) is not finally established until a descent rate of $\overline{\mu}_z \approx 0.7$.

In free flight, thrust settling is usually offset by an appropriate change to the collective pitch of the rotor blades. In this case, the flow dynamics associated with thrust settling appear instead as an increase in the torque required by the rotor, as shown in Fig. 11 for a simulation of Gao's rotor, flown along the same trajectory as before, but this time trimmed throughout to a constant mean thrust coefficient of 0.0073. Figs. 12 and 13 , showing the blade loading and velocity normal to the blade in the case of constant $C_T$, reveal that the aerodynamic effect of the wake upon the rotor blades is similar to when the rotor is flown at constant collective pitch, with the important difference that the thrust on the rotor is maintained by a significant increase in the loading on the inboard sections of the blade as the

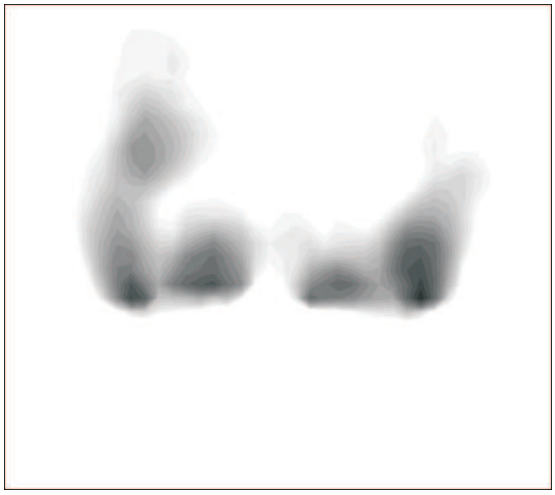

Figure 18: *Averaged wake geometry at* $\overline{\mu}_z = 1.15$.

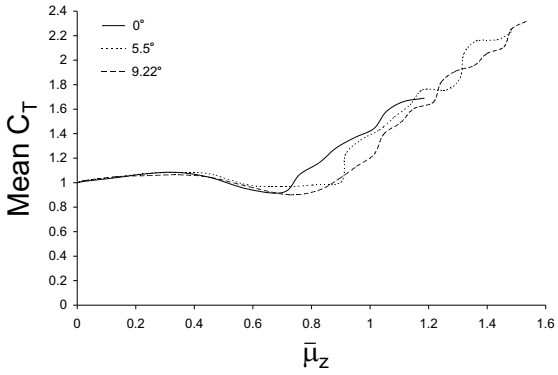


Figure 19: *Mean thrust vs. descent rate: comparison between rotors with different twist rates.*

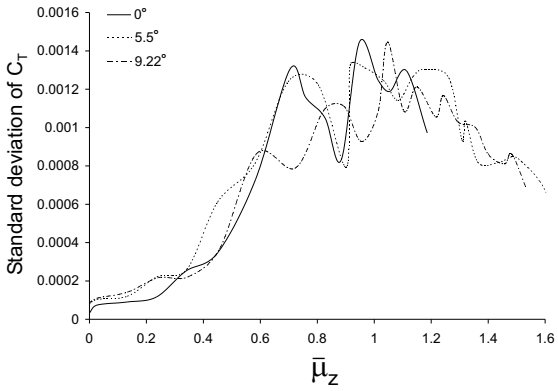


Figure 20: *Standard deviation of thrust vs. descent rate: comparison between rotors with different twist rates.*

controller increases the collective pitch of the blades to compensate for the loss of lift on the outboard sections of the blade.

It remains to relate the increase in inflow at the outer sections of the blades during the onset of thrust settling to changes in the structure of the wake. To this end, it is possible from the output of the VTM to measure the changes in the strength of the wake within specified regions of the flow field surrounding the rotor. This method was first used by Ahlin and Brown (Ref. 2) where, as a direct measure of the fluid dynamics of the wake system, it proved to be a very useful indicator of VRS initiation. For convenience, define the *wake intensity* as the integral of the vorticity magnitude over a specified volume of the flow. Fig. 14 compares the wake intensity, for Gao's rotor flown at constant collective pitch, in a box-shaped domain located just below the rotor to the wake intensity in a box-shaped domain enclosing the flow immediately above the rotor. In this figure, the wake intensities in each of the domains have been normalised by dividing through by the wake intensity in the union of the two domains under hovering conditions. During the initial stages of the descent, i.e. for $\overline{\mu}_z < 0.3$, the wake intensity beneath the rotor increases in approximately linear fashion, representing a smooth, uninhibited compression of the wake, or, in other words, a gradual bunching together of the vortex filaments immediately below the rotor. At $\overline{\mu}_z = 0.3$, the wake intensity below the rotor jumps suddenly, and at the same time, a significant level of vorticity appears for the first time above the rotor. The wake intensity below the rotor remains roughly constant until $\overline{\mu}_z \approx 0.45$, but the appearance of fluctuations in the wake intensity of relatively large amplitude compared to the mean is consistent with the first appearance of significant disturbances in the structure of the wake near to the rotor. Comparing Fig. 14 and Fig. 6 shows that the change in character of the wake intensity below the rotor at $\overline{\mu}_z = 0.3$ marks also the earliest onset of notable unsteadiness in the thrust produced by the rotor. As the descent rate is increased beyond $\overline{\mu}_z = 0.45$, the wake intensity both above and below the rotor increases rapidly, and the fluctuations in the wake intensity become steadily more extreme. The onset of thrust settling coincides with the beginning of this regime. Fig. 15 compares the wake intensity in a domain that envelops the rotor from the mid-span outwards with the wake intensity in a volume that encloses the remaining internal sections of the near-rotor flow field. Again, the wake intensities shown in this figure are normalised by the wake intensity in the union of the two domains under hovering conditions. It is clear that the increase in the wake intensity between $\overline{\mu}_z = 0.45$ and $\overline{\mu}_z = 0.5$ is confined to the outboard parts of the rotor, suggesting that, when viewed in conjunction with the wake images of Fig. 7, the onset of thrust settling is caused by the increase in downwash velocity that is induced by the compression of the tip vortices beneath the outboard part of the rotor, rather than by any gross change in the characteristics of the flow.

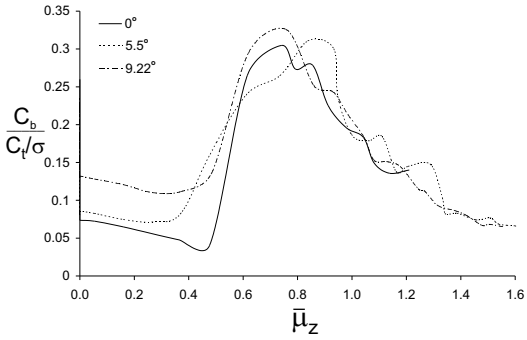


Figure 21: *Blade loading at* 0.2*R (normalised by* $C_T/\sigma$*) vs. descent rate: comparison between rotors with different twist rates.*

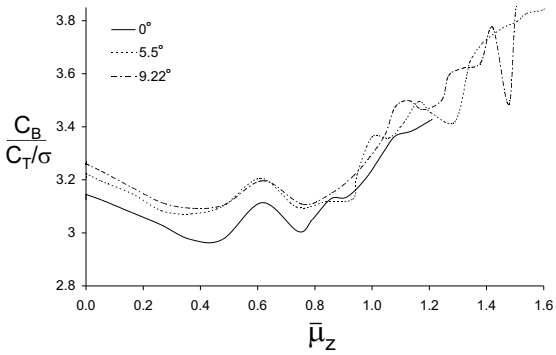


Figure 22: *Blade loading at* 0.7*R (normalised by* $C_T/\sigma$*) vs. descent rate: comparison between rotors with different twist rates.*

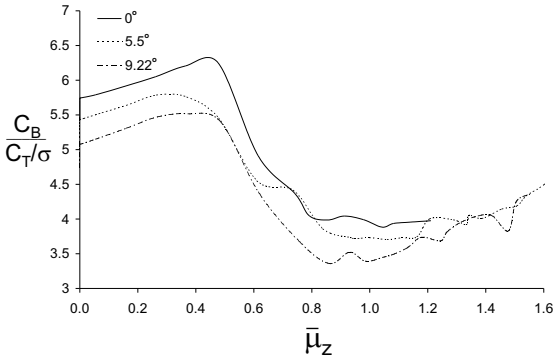


Figure 23: *Blade loading at* 0.9*R (normalised by* $C_T/\sigma$*) vs. descent rate: comparison between rotors with different twist rates.*

The rapid increase in the wake intensity both below and above the rotor as the descent rate is increased beyond $\overline{\mu}_z = 0.5$ occurs simultaneously with the breakdown of the orderly structure of the wake and the appearance of the toroidal flow that is characteristic of the fully-developed VRS. For descent rates greater than $\overline{\mu}_z \approx 0.7$, the wake intensity above the rotor increases at the expense of the wake intensity below the rotor, indicating a shift in the toroidal vortex structure from below to above the rotor. The crossover point at $\overline{\mu}_z \approx 0.8$ coincides with the maximum intensity of the thrust fluctuations experienced by the rotor and also with the maximum depth of the thrust settling regime. Thus, although thrust settling is brought about by the compression of the rotor wake while it is still in its low-speed, tubular form, it is certainly deepened and sustained by the collapse of the wake into the toroidal form found in the fully developed VRS. Figs. 16, 17 and 18 show this shift in the position of the toroidal vorticity field that engulfs the rotor, and correlation of Fig. 6 with Fig. 17 shows that thrust recovery on the rotor begins once the toroidal VRS wake begins to lift clear of the rotor. Also shown, at the highest descent rates, is the beginning of the process whereby disturbances are once again swept downstream into the far field, accompanied by the eventual cessation of VRS activity as the relatively orderly wake structure of the windmill brake state is established.

## The Effect of Blade Twist

A concern to the designers of conventional rotorcraft is that a small change in one or more of the design parameters of the rotor might result, because of the highly nonlinear character of the flow physics governing the VRS, in a disproportionate change in the performance of the system. Several previous works (Ref. 15) have implicated blade twist as one of the most important design variables influencing the rotor behaviour once within the VRS, but little is known about the sensitivity of rotor performance in the VRS to changes in this parameter.

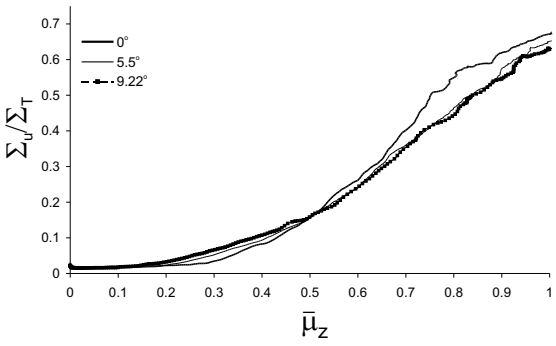


Figure 24: *Fraction of wake intensity above the rotor vs. descent rate: comparison between rotors with different twist rates.*

Gao's experiments included an investigation of the effect of moderate levels of blade twist (i.e. $0^\circ - 10^\circ$) on the behaviour of rotors in the VRS. He concluded that twist had little influence on the descent rate at which the VRS was initiated, but that, within the VRS, there was a noticeable effect on the amplitude of the thrust and torque fluctuations experienced by the rotor. In this section, Gao's experiments are replicated using the VTM to try to understand the aerodynamic origins of any sensitivity in rotor behaviour in the VRS to changes in the twist of the blades. The behaviour of rotors with blade twists of $0^\circ$, $5.5^\circ$ and $9.22^\circ$, and with the same planform and teetering configuration as Gao's rotors, are contrasted. As before, the range of descent rates of interest was traversed by subjecting the rotor to a small vertical acceleration while holding fixed the collective pitch. The thrust coefficient produced at hover was 0.00735 in all cases.

Figures 19 and 20 show the variation with descent rate of the mean, and the standard deviation, of the thrust produced by the rotors. Fig. 19 shows that the descent velocity at which thrust settling begins is confined to a very small range of descent rates, nominally just before $\overline{\mu}_z = 0.5$, and thus confirms Gao's observation that the onset of the VRS is only weakly affected by blade twist. The same figure show a reasonably significant influence of twist on the breadth of the thrust settling regime, however. The rotor with untwisted blades appears to recover the thrust level achieved prior to thrust settling at a lower descent rate than the other two rotors, the last rotor to recover being the one with the most highly twisted blades. Fig. 20 shows that a marginally higher peak fluctuation amplitude is experienced by the rotor with untwisted blades, and that the rotor with the most highly twisted blades experiences its peak thrust fluctuation at somewhat higher descent rates than the other two rotors. These effects are rather subtle, and it is debatable whether the differences in behaviour between the rotors would be operationally significant.

Figures 21, 22 and 23 show the variation of blade loading with descent rate for the three rotors. The data in the figures has been normalised by $C_T/\sigma$ to allow any spanwise redistribution in blade loading with descent rate to be more clearly visualised. Whilst all three rotors show much the same qualitative trends as described earlier in the context of thrust settling, there are also some small quantitative differences between the blade loading distributions on each of the rotors. As expected, these appear to be associated primarily with the increase in the loading on the inboard sections of the rotor as the twist of the blades is increased. The one significant difference is in the rate of recovery of the loading on the outboard part of the blades. This feature is responsible for the earlier thrust recovery, post-VRS, of the rotor with untwisted blades compared to the rotors with twisted blades, as shown in Fig. 19. Fig. 24 shows the relative division of wake intensity between the flow above and below the rotors and illustrates quite clearly that, in the case of the rotor with untwisted blades, the wake moves more suddenly from below to above the rotor during the later stages of the development of the VRS. It is not entirely clear at this stage what causes this difference in behaviour, but quite conceivably the small differences in loading, and hence inflow distribution along the blades, could yield a subtly different trajectory of the toroidal VRS flow as it moves from below the rotor to above, but the effect is too small to be seen in the results presented here. Finally, Fig. 25 shows the variation of the fluctuating component of the loading along the span of the blades as a function of descent rate. Although the

fluctuations begin at the root of the blade, it is clear that they quickly spread to engulf the entire length of the blade with almost uniform amplitude as the rotor enters the fully developed VRS.

The data presented here suggests that, at least for moderately twisted blades, the influence of twist on the behaviour of the rotor, both in terms of its mean thrust performance and in terms of the levels of unsteady loading generated by the system when in the VRS, is relatively minor. This conclusion should provide some confidence to the designers of conventional rotorcraft, but the trend in modern rotor designs is to use somewhat higher levels of blade twist than those analysed here. It seems imprudent to extend the current analysis to these systems, however, until properly validated models become available that can be used with confidence to predict those aspects of stall behaviour that are peculiar to highly twisted rotor blades.

## The Influence of Blade Stall

Indeed, it has been suggested by several authors (Ref. 15) that blade stall may be an essential component of the flow physics during VRS. While it is quite feasible that localised stall might have an effect on the behaviour of the inboard segments of the blade, it is thought unlikely that global stall of the rotor plays a role in VRS for any sensible values of the rotor operating thrust. A worry, though, is that, especially for the case of experiments conducted at constant collective pitch, the angles of attack induced on the inboard portions of blades at the highest descent rates may indeed be sufficient to generate an extended region of stalled flow on the rotor. If this is the case, then, for instance, the use of experimental data generated under conditions of constant collective pitch to understand the behaviour of the flight article, where the more common operating condition is to fly the rotor at very close to constant thrust coefficient, becomes very suspect. In this section the aerodynamic conditions on the same rotors that were used to investigate the effects of blade twist are examined to reveal the extent of the region of stalled flow on the rotor blades. The aerofoil model used in the simulations contains a full 360° $C_L$-$\alpha_e$ dependency similar to that of the NACA0012 type blade section, and thus is capable of representing some of the effects of static stall on the behaviour of the rotor.

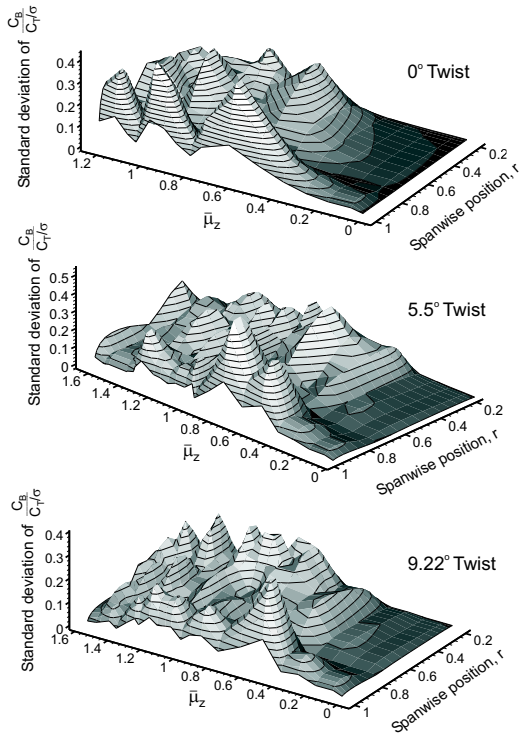


Figure 25: *Spanwise variation in the standard deviation of the blade loading (normalised by $C_T/\sigma$) vs. descent rate: comparison between rotors with different twist rates.*

Fig. 26 shows the simulated variations of effective angle of attack $\alpha_e$ and local lift coefficient $C_L$ along the length of Gao's most highly twisted rotor blade. Inspection of the behaviour of the lift coefficient with descent rate at $0.2R$, shows the onset of significant nonlinearity in the relationship between $C_L$ and $\alpha_e$, and thus, by inference, blade stall, at a descent speed of $\overline{\mu}_z \approx 0.7$. Thus, at least in the case where the blade twist rates are moderate, VRS onset occurs before blade stall, or, conversely, blade stall

can have no effect on the descent rate for VRS onset. It is still possible though that stall could influence the subsequent development of the VRS. Brown and Leishman *et al.* (Ref. 15) postulated that, at least on highly loaded, highly twisted blades, stall acts to reduce the thrust fluctuations generated by the rotor because of the degraded sensitivity of the aerofoil sections to changes in $\alpha_e$ when they operate in the non-linear region of the $C_L$-$\alpha_e$ curve. The results presented here suggest that this argument can be extended to the behaviour of rotors where the incidence on the inboard parts of the blade becomes very large, for instance in wind tunnel tests conducted at constant collective pitch with no direct control over the thrust produced by the rotor. Inspection of Fig. 26 shows that, even with the collective pitch held fixed, stall never propagated further outboard than about 40% of the rotor radius over the entire descent range that was simulated. Yet Fig. 25 shows that appreciable VRS-induced fluctuations in the loading are indeed generated within this region of the rotor. This suggests that, even when the blades of the rotor are only moderately twisted, the form of the aerodynamic response within the inner region of the rotor, particularly with regards to the behaviour of these elements of the blades near and post-stall, may play a significant role in governing the dynamic behaviour of rotors tested in this way, at least at higher descent rates within the VRS. The results presented here thus caution against overly direct extrapolation of the results of such tests to the behaviour of the full-scale article, similarly in comparing results from experiments conducted at constant collective pitch against results obtained, for instance, at constant thrust coefficient. The root of the problem, as is illustrated particularly well by comparing Figs. 8 and 12 of this paper, is that the conventional process of non-dimensionalisation of the descent rate with respect to the extrapolated induced velocity at hover, which is required to convert the one type of data into a form that is compatible with the other, is capable of hiding rather gross differences in loading distribution at different operating conditions even when the blades are geometrically similar.

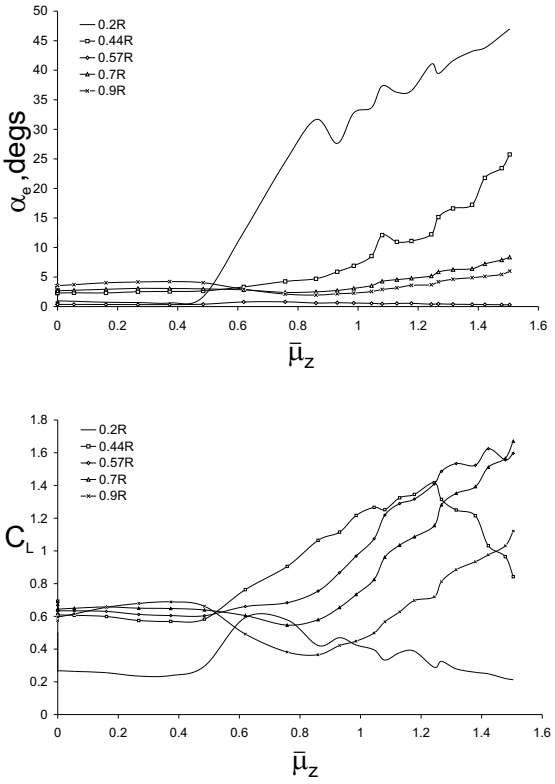


Figure 26: *Spanwise variation in angle of attack and lift coefficient vs. descent rate for the rotor with blades having* $9.22^\circ$ *of twist.*

# Conclusions

Simulations of the behaviour in descending flight of a series of rotors having a moderate degree of blade twist were conducted using Brown's VTM computational model. Correlation with the experimental data of Washizu *et al.* (Ref. 10) and Gao (Ref. 17) is presented to lend credence to the ability of the VTM to yield reasonably good predictions of the behaviour of rotors in the VRS.

Simulations using the VTM show the onset of thrust settling on the rotor to occur before the wake of the rotor has fully transitioned from its tubular, hover-like form into the toroidal topology of the fully-developed VRS. The initial cause of thrust settling is a significant loss of loading on the most outboard portions of the rotor, and this is most likely induced by compaction of the tip vortices below the plane of the rotor at moderate, pre-VRS descent rates. The

regime of thrust settling persists as the wake collapses into its toroidal VRS topology. Recovery of the rotor thrust begins as the toroidal structure of the VRS lifts above the rotor, but this change in behaviour of the rotor occurs at descent rates well below that at which the relatively orderly wake structure of the windmill brake state is established.

The behaviour of the rotor in the VRS is practically insensitive to variation of the blade twist, at least for moderate twist values ($0^\circ - 10^\circ$). Simulations show negligible effect of twist on the descent rate for VRS onset, but subtle effects on the amplitude of thrust fluctuations in the VRS and on the descent rate at which thrust recovery on the rotor begins. Although stall appears to play a negligible role in influencing the descent rate for VRS onset, it is possible under specific circumstances that stall on the inner parts of the blades may significantly modify the behaviour of the rotor at higher descent rates within the VRS. This needs to be borne in mind particularly when data from dissimilarly-conducted wind tunnel tests is compared, or when certain, supposedly generic, wind tunnel data is extrapolated to the behaviour of the full-scale helicopter in flight.

## Acknowledgements

The work described in this paper is partially supported by the ongoing U.K. Engineering and Physical Sciences Research Council Grant GR/R/90116/01 “Understanding the Fluid Dynamics of Rotor Wake Breakdown in Low Speed Flight”.

## References

[1]Bhagwat, M.J., and Leishman, J.G., “Stability Analysis of Rotor Wakes in Axial Flight,” *Journal of the American Helicopter Society*, Vol. 45, No. 3, 2000, pp. 165–178.

[2]Ahlin, G.A., and Brown, R.E., “Predicting the Onset of the Vortex Ring State under Accelerated Flight Conditions,” 61st American Helicopter Society Annual Forum, June 2005, Grapevine, Texas.

[3]Newman, S.J., Brown, R., Perry, F.J., Lewis, S., Orchard, M., and Modha, A., “Predicting the Onset of Wake Breakdown for Rotors in Descending Flight,” *Journal of the American Helicopter Society*, Vol. 48, No. 1, 2003, pp. 28–38.

[4]Yaggy, P.F., and Mort, K.W., “Wind-Tunnel Tests of Two VTOL Propellers in Descent,” NASA TN D-1766, March 1963.

[5]Castles, Jr., W., and Gray, R.B., “Empirical Relation between Induced Velocity, Thrust, and Rate of Descent of a Helicopter Rotor as Determined by Wind-Tunnel Tests on Four Model Rotors,” NASA TN-2474, October 1951.

[6]Green, R.B., Gillies, E.A., and Brown, R.E., “The Flow Field around a Rotor in Axial Descent,” *Journal of Fluid Mechanics*, Vol. 534, 2005, pp. 237-261.

[7]Drees, J., and Hendal, W., “Airflow Patterns in the Neighbourhood of Helicopter Rotors,” *Journal of Aircraft Engineering*, Vol. 23, No. 26, 1951, pp.107–111.

[8]Stack, J., Caradonna, F., and Savas, O., “Flow Visualizations and Extended Thrust Time Histories of Rotor Vortex Wakes in Descent,” 4th American Helicopter Society Decennial Specialists’ Conference on Aeromechanics, January 2004, San Francisco, California.

[9]Azuma, A., and Obata, A., “Induced Flow Variation of the Helicopter Rotor Operating in the Vortex Ring State,” *Journal of Aircraft*, Vol. 5, No. 4, 1968, pp. 381–386.

[10]Washizu, K., Azuma, A., Koo, J., and Oka, T., “Experiments on a Model Helicopter Rotor Operating in the Vortex Ring State,” *Journal of Aircraft*, Vol. 3, No. 3, 1966, pp. 225–230.

[11]Glauert, H., “The Analysis of Experimental Results in the Windmill Brake and Vortex Ring States of an Airscrew,” Aeronautical Research Committee R&M No. 1026, Februry 1926.

[12]Johnson, W., “Model for Vortex Ring State Influence on Rotorcraft Flight Dynamics,” American Helicopter Society 4th Decennial Specialists’ Conference on Aeromechanics, San Francisco, January 2004.

[13]Brown, R.E., “Rotor Wake Modeling for Flight Dynamic Simulation of Helicopters,” *AIAA Journal*, Vol. 38, No. 1, 2000, pp. 57–63.

[14]Brown, R.E, and Line, A.J., “Efficient High-Resolution Wake Modeling using the Vorticity Transport Equation,” *AIAA Journal*, Vol. 43, No. 7, 2005, pp. 1434–1443.

[15]Brown, R.E., Leishman, J.G., Newman, S.J., and Perry, F.J., “Blade Twist Effects on Rotor Behaviour in the Vortex Ring State,” 28th European Rotorcraft Forum, Bristol, September 2002.

[16]Brown, R.E., Line, A.J., and Ahlin, G.A., “Fuselage and Tail-Rotor Interference Effects on Helicopter Wake Development in Descending Flight,” 60th American Helicopter Society Annual Forum, June 2004, Baltimore, Maryland.

[17]Gao, Z., “New Achievements in Helicopter Aerodynamics,” *Aviation Industry Publications*, 1999 (Translated from Chinese to English by Chan, W., 2003)